

USING GAMMA-RAY, NEUTRON, AND SPECTRAL REFLECTANCE DATA TO OBTAIN ACCURATE MEASURES OF GLOBAL LUNAR IRON ABUNDANCES. J. J. Hagerty¹, D. J. Lawrence², J. J. Gillis-Davis³, J. T. S. Cahill², and R. Klima², ¹U.S.G.S. Astrogeology Science Center, Flagstaff, AZ 86001 email: jhagerty@usgs.gov, ²The Johns Hopkins University, Applied Physics Laboratory, Laurel, MD, ³University of Hawai'i, Hawai'i Institute of Geophysics and Planetology, Honolulu, HI.

Introduction: Accurate knowledge of iron abundance in lunar materials is the foundation for various types of lunar science studies. For instance, iron is a key element for testing fundamental theories of lunar formation and evolution such as the magma ocean hypothesis [e.g., 1, 2]. Iron also tends to be a primary discriminator of lunar basaltic and non-basaltic materials. For example, Lucey and Jolliff et al. [3, 4] used lunar sample data as a key discriminator to distinguish between different types of lunar terrains. Finally, iron abundance can be combined with other major element abundance information to infer important information about the Moon. For example, the relationship between iron and magnesium abundance can be used to determine the chemical evolution of a magma and to make inferences about basalt petrogenesis. This includes the composition of the mantle source region from which the basalts were derived [e.g., 3, 5].

Multiple algorithms have been derived to estimate the abundance of iron from two portions of the electromagnetic spectrum (gamma-ray and UV-visible-near-IR spectral reflectance). These algorithms have been applied to Lunar Prospector gamma-ray (LP-GRS) and Clementine spectral reflectance (CSR) data sets to yield maps of global lunar Fe abundance. While these two data products are in relative agreement for a large portion of the lunar surface, there are significant discrepancies for many locations [6, 7]. In some cases, these discrepancies are large enough (i.e., up to 11 wt.% different) to lead to different conclusions regarding important lunar science questions. The divergence in estimated Fe in these locations may provide new information about the composition and physical properties of surface materials, which in turn may have implications about the evolution of the Moon.

Recent Progress and Reworked Methodology: A first step toward understanding these divergent areas is to determine if these discrepancies are the result of different resolutions of the two instruments (i.e., Clementine footprint is 100-200 m/pixel and Lunar Prospector GRS footprint is >50 km/pixel). Initial analyses of data smoothing techniques suggest that the majority of spatial discrepancies do not result from a spatial footprint mismatch [8]. Instead, the discrepant Fe estimates result from either inherent differences in how each technique estimates composition or the physical character of the lunar surface [9].

Three potential sources for the discrepancies between the iron data products remain: 1) Footprint/resolution issues, 2) spectral algorithm limitations, 3) sampling depth, and/or 4) mineralogy composition/mixing. To address these issues we are attacking the problem from a few different angles by more closely examining the influence of neutrons on gamma ray data, reevaluating spectral algorithms relative to mineral absorption coefficients, and forward modeling of gamma ray data.

Fast Neutron Estimates of Iron: Fast neutrons are highly sensitive to variations in average atomic mass, which is dominated by Fe and Ti abundances in lunar materials [10, 11]. In Lawrence et al. [6], it was concluded that discrepancies within South Pole-Aitken (SPA) basin between LP-GRS and CSR Fe estimates were due to mineralogical differences between nearside and SPA basin materials. Since Ti abundances within SPA basin are quite low, fast neutrons can provide an independent measure of Fe within SPA basin. Based on mutual correlations between fast neutrons, LP-GRS Fe, and CSR Fe measured abundances (Figures 1 and 2), we find that the GRS-derived data are consistent with fast neutrons (Figure 1), but that CSR-derived data overestimate Fe abundances by ~2 wt.%. These results are consistent with prior conclusions by Lawrence et al. [6] and provide additional evidence that there are composition and/or physical property effects within SPA basin that are responsible for the discrepancies.

Spectral Algorithms: A variety of studies have been carried out using spectral reflectance data to obtain global estimates of iron abundance [2, 12-16]. These studies developed empirical algorithms using the Clementine eleven-band UVVIS-near-IR data set to determine estimates of iron abundance for a wide variety of lunar terrains. Several of these studies determined that spectral reflectance data are sensitive to a variety of effects (e.g., soil maturity, grain size, mineralogy) that cause qualitative and quantitative uncertainties in the determination of iron abundances.

A preliminary survey of the FeO incongruities [3, 6] suggested that several of the discrepancies are located adjacent to regions containing complex lithologic assemblages. While it is suggested that these regions tend to consist dominantly of mafic lithologies [3, 6, 17], we find that there are definable correlations between mineral abundance estimates and iron abundance differences [8, 9]. Our next goal is to differentiate how

much of these correlations are due to algorithm limitations are inherent to certain mineral species measured using spectral reflectance.

Forward Modeling: As part of our forward modeling process, we model a portion of the lunar surface in which we can control the Fe abundances of specific geologic features. We select our regions of interest using a combination of existing geologic maps, orbital photography, spectral reflectance data, and gamma-ray and neutron data [e.g., 18, 19]. We use these data to define specific geologic features and lithology types.

After identifying major geologic units in our model, we assign Fe abundances to each of those units using the procedures outlined in our previous work [e.g., 18, 19]. We propagate the expected gamma-ray flux from these geologic features through the LP-GRS spatial response, which produces a simulated Fe distribution. We then compare the simulated Fe distribution to the measured Fe data and iteratively adjust the simulated distribution until we achieve a match with the measured data. Once a match is achieved, we can use the modeled Fe distribution to determine the Fe abundance of any given feature of interest.

Results and Conclusions: Initial results from our investigation include:

- Significant differences in FeO estimates appear to be due to limitations of multispectral data reduction algorithms.
- Spectral reflectance data reduction algorithms overestimate FeO abundance in highly mafic regions. However, no one mafic mineral appears to be the source of the discrepancy.
- The FeO difference improves as plagioclase + olivine abundance increases and pyroxene abundance decreases. However, previous studies suggest plagioclase + olivine mixtures cause spectral reflectance algorithms to underestimate FeO [i.e., 3]. A logical next step is to investigate these correlations using data from Moon Mineralogy Mapper.
- GRS-derived data are consistent with fast neutrons (Fig. 1), while CSR-derived data overestimate Fe abundances by ~2 wt.% (Fig. 2).
- Gamma-ray estimates tend to overestimate FeO in more feldspathic highlands regions.
- Forward modeling of FeO abundances in basalts within SPA basin, indicate that lithologic mixing, indistinguishable in the low resolution LP-GRS data, causes the GRS FeO data to be underestimated in these basalts.

Acknowledgements: This work was supported by NASA through Lunar Advanced Science and Exploration Research Program grant NNN09AL71I.

References: [1] Warren P. H. (1985) *An. Rev. Earth Planet. Sci.*, 13, 201; [2] Lucey P. G. et al. (1995) *Science*, 268, 1150; [3] Lucey P. G. (2006) *J. Geophys. Res.*, 111; [4]

Jolliff B. L. et al. (2000) *J. Geophys. Res.*, 105, 4197; [5] Hess P. C. (1989) *Origins of Igneous Rocks*, Harvard Univ. Press, Cambridge, 336; [6] Lawrence D. J. et al. (2002) *J. Geophys. Res.*, 107; [7] Gillis J. J., Jolliff B. L., and Korotev R. L. (2004) *Geochim. Cosmochim. Acta*, 68, 3791; [8] Hagerty J. J. et al. (2010) *NASA Lunar Science Forum*; [9] Cahill J. T. S. et al. (2010) *2010 AGU Fall Meeting*; [10] Maurice S. et al. (2000) *J. Geophys. Res.*, 105, 20365; [11] Gagnault O. et al. (2001) *Geophys. Res. Lett.*, 28, 3797; [12] Lucey P. G. et al. (1998) *J. Geophys. Res.*, 103, 3701; [13] Lucey P. G. et al. (2000) *J. Geophys. Res.*, 105, 20297; [14] Blewett D. T. et al. (1997) *J. Geophys. Res.*, 102, 16319; [15] Le Mouelic S. et al. (2002) *J. Geophys. Res.*, 107; [16] Wilcox B. B. et al. (2005) *J. Geophys. Res.*, 110; [17] Pieters C. M. et al. (2001) *J. Geophys. Res.*, 106, 28001; [18] Hagerty J. J. et al. (2006) *JGR*, 111; [19] Hagerty J. J. et al. (2009) *J. Geophys. Res.*, 114.

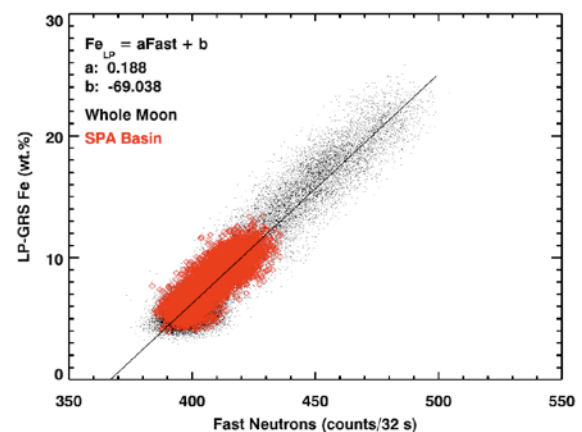


Figure 1. Plot of fast neutrons (counts) versus LP-GRS Fe (wt.%), demonstrating a strong linear relation consistent with fast neutron dependence on average atomic mass.

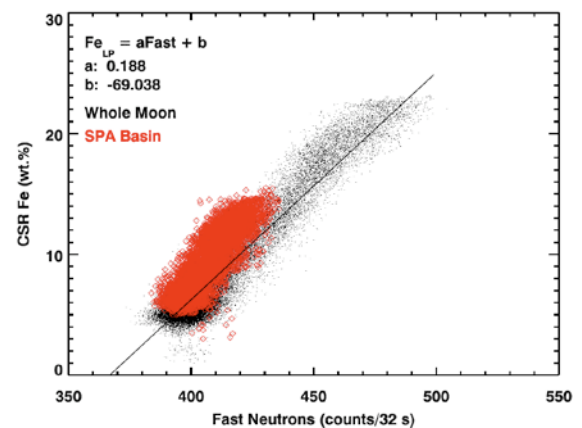


Figure 2. Plot of fast neutrons (counts) versus CSR Fe (wt.%), demonstrating that FeO abundances in SPA basin are not consistent with the linear correlation from Figure 1.